

Electronic structure induced by lateral composition modulation in GaInAs alloys

T. Mattila, L. Bellaiche, L.-W. Wang, and Alex Zunger

Citation: [Applied Physics Letters](#) **72**, 2144 (1998); doi: 10.1063/1.121303

View online: <http://dx.doi.org/10.1063/1.121303>

View Table of Contents: <http://scitation.aip.org/content/aip/journal/apl/72/17?ver=pdfcov>

Published by the [AIP Publishing](#)

Articles you may be interested in

[Density functional theory simulations of amorphous high- \$\kappa\$ oxides on a compound semiconductor alloy: a-Al₂O₃/InGaAs\(100\)-\(4×2\), a-HfO₂/InGaAs\(100\)-\(4×2\), and a-ZrO₂/InGaAs\(100\)-\(4×2\)](#)

[J. Chem. Phys.](#) **135**, 244705 (2011); 10.1063/1.3657439

[Effect of interface structure on the optical properties of InAs/GaSb laser active regions](#)

[Appl. Phys. Lett.](#) **80**, 1683 (2002); 10.1063/1.1456238

[Theoretical performance and structure optimization of 3.5–4.5 \$\mu\$ m InGaSb/InGaAlSb multiple-quantum-well lasers](#)

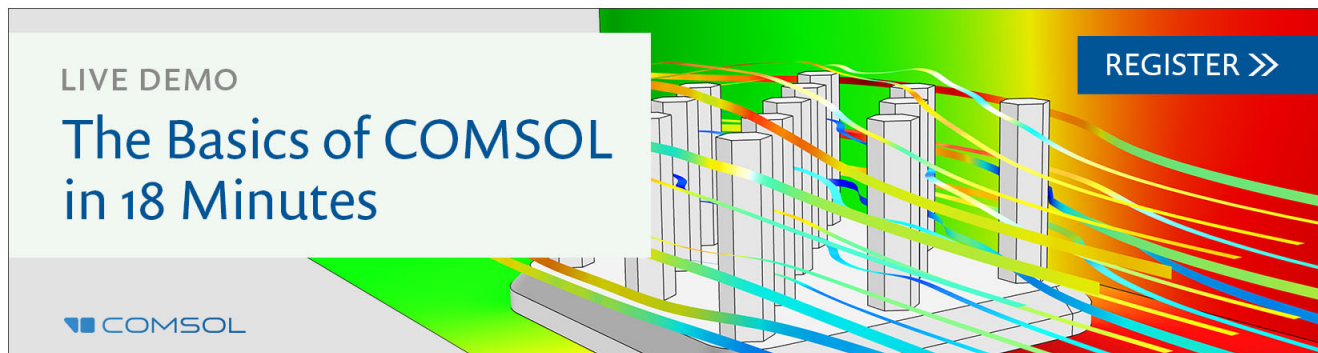
[Appl. Phys. Lett.](#) **78**, 2640 (2001); 10.1063/1.1369146

[The structural, chemical, and electronic properties of a stable GaS/GaAs interface](#)

[J. Appl. Phys.](#) **86**, 6940 (1999); 10.1063/1.371776

[Band structure and confined energy levels of the Si₃N₄/Si/GaAs system](#)

[J. Appl. Phys.](#) **82**, 275 (1997); 10.1063/1.365808

A promotional banner for COMSOL software. On the left, a white box contains the text 'LIVE DEMO' and 'The Basics of COMSOL in 18 Minutes'. The COMSOL logo is at the bottom left. The background features a 3D model of a multi-layered structure with colorful streamlines (red, yellow, green, blue) flowing through it. A blue button with white text 'REGISTER >>' is located in the top right corner.

LIVE DEMO

The Basics of COMSOL in 18 Minutes

COMSOL

REGISTER >>

Electronic structure induced by lateral composition modulation in GaInAs alloys

T. Mattila,^{a)} L. Bellaiche,^{b)} L.-W. Wang, and Alex Zunger^{c)}
National Renewable Energy Laboratory, Golden, Colorado 80401

(Received 13 January 1998; accepted for publication 27 February 1998)

It has been recently shown that growth of [001]-oriented short period $(AC)_n/(BC)_n$ vertical superlattices ($n \sim 1-2$) spontaneously creates a lateral composition modulation in the substrate plane ([110] direction), where wire-like AC-rich and BC-rich domains alternate with a period of $\sim 100-200$ Å. This creates a new type of lattice structure with orthogonal [001] and [110] strain fields and compositional waves. Using a three-dimensional plane-wave pseudopotential approach, we study here the electronic properties of this type of structure in a GaInAs alloy, predicting valence band splittings into distinctly polarized components, a ≤ 100 meV band-gap reduction and strong, type I electron and hole confinement in the In-rich lateral channels. © 1998 American Institute of Physics. [S0003-6951(98)02817-4]

When a short-period superlattice (SPS) of $(\text{GaP})_n/(\text{InP})_n$ ¹⁻⁴ or $(\text{InAs})_n/(\text{GaAs})_n$ ⁵⁻⁷ or $(\text{AlAs})_n/(\text{InAs})_n$ ⁷⁻⁹ are grown intentionally along the [001] direction with period $n = 1-2$ monolayers, an unintentional, lateral composition modulation develops spontaneously in the substrate plane ([110] or $\bar{1}10$ directions) with a surprisingly long coherence length. Typically, the lateral modulation has a periodicity of $\lambda \sim 100-200$ Å, the composition fluctuates by $\sim 10\%$ about the average value, and the band gap is redshifted by $\sim 100-300$ meV with respect to a random alloy of equivalent composition. In all cases, the photoluminescence exhibits a strong polarization anisotropy with respect to the [110] and $\bar{1}10$ directions: in general, polarization orthogonal to the modulation direction is strongly enhanced over that in the parallel direction.^{2-4,7,9} This lateral composition modulation (CM) is distinct from the vertical [001] platelet modulation occurring in growth of, e.g., InAsSb (Ref. 10) or InAlAs (Ref. 11), or from the CuPt-like spontaneous ordering¹² occurring along the [111] direction with monolayer periodicity. Lateral CM, vertical CM and spontaneous ordering were all reviewed in Ref. 12.

Lateral composition modulation creates a new type of lattice structure in which nearly sinusoidal [110] translational symmetry with periodicity of ~ 20 lattice constants coexists with a $\sim 1-2$ monolayer periodicity in the orthogonal [001] direction. This structure thus exhibits an interference from two orthogonal strain fields, superimposed on two corresponding compositional waves. Previous descriptions of such effects⁴ ignored the explicit strain and explicit vertical short-period monolayer structure, considering it instead as a pseudo-alloy,¹¹ while treating the lateral modulation within a simplified $\mathbf{k} \cdot \mathbf{p}$ approach with one-dimensional strain. While inclusion of the vertical monolayer structure within a $\mathbf{k} \cdot \mathbf{p}$ description is technically possible, this effective-mass based approach breaks down¹³ for superlattices of such short (~ 1

-2 monolayer) period encountered here. Here we provide a full three-dimensional band structure description of lateral composition modulation structures, clarifying the role of amplitude, periodicity and orientation on the energy levels, polarization and wave function localization. We use a direct-diagonalization pseudopotential plane-wave approach for the electronic structure,¹⁴ while obtaining the three-dimensional strain field from minimizing the strain energy in an atomistic (rather than continuum) description.^{15,16}

Atomic structure and strain fields: In this study we concentrate on modeling a $n = 1.5$ SPS. The assumed sequence of cation monolayers along [001] is $[\text{Ga}_1/\text{Ga}_{0.5}\text{In}_{0.5}/\text{In}_1/\dots]$. Note that in this SPS structure the second layer is mixed; if this layer segregates, lateral CM results automatically. Having specified the [001] periodicity, we next construct the simulation cell which exhibits compositional waves in the [110] direction. We select m_3 (110) planes, each containing m_1 atoms in the $\bar{1}10$ direction and m_2 atoms in the [001] direction. The planar composition $x(\mathbf{R})$ for the \mathbf{R} th (110) $\text{Ga}_{1-x}\text{In}_x$ plane will follow

$$x(\mathbf{R}) = x_0 \left(1 + A \sin \frac{\mathbf{R} \cdot \mathbf{u}}{\lambda} \right), \quad (1)$$

where x_0 is the sample-average composition about which $x(\mathbf{R})$ fluctuates, A is the fluctuation amplitude, \mathbf{u} is its direction and λ is its wavelength. For $\lambda = 149$ Å we have a total of $2 \times m_1 \times m_2 \times m_3 = 2 \times 20 \times 9 \times 72 = 25920$ atoms for $n = 1.5$. Having created these composition profiles along the vertical and lateral direction by specifying $\{n, A, x_0, \lambda, \mathbf{u}\}$, we next permit all atomic positions to relax, so as to minimize the three-dimensional strain energy. We do so by minimizing the valence force field (VFF) energy¹⁶ that includes bond-stretching and bond-bending forces (this atomistic technique differs¹⁵ from continuum elasticity). The resulting minimum-energy atomic positions are illustrated in Fig. 1 for $n = 1.5$, $A = 16.7\%$, $x_0 = 0.50$, $\lambda = 149$ Å and $\mathbf{u} = [110]$. Note that the individual planes are buckled. To see this more clearly, Fig. 2 illustrates the main atomic displacements. Figures 2(a) and 2(b) show the change in inter-row distance between the

^{a)}Electronic mail: tmattila@sst.nrel.gov

^{b)}Present address: Rutgers University, Dept. of Physics and Astronomy, P.O. Box 849, Piscataway, NJ 08855-0849.

^{c)}Electronic mail: alex_zunger@nrel.gov

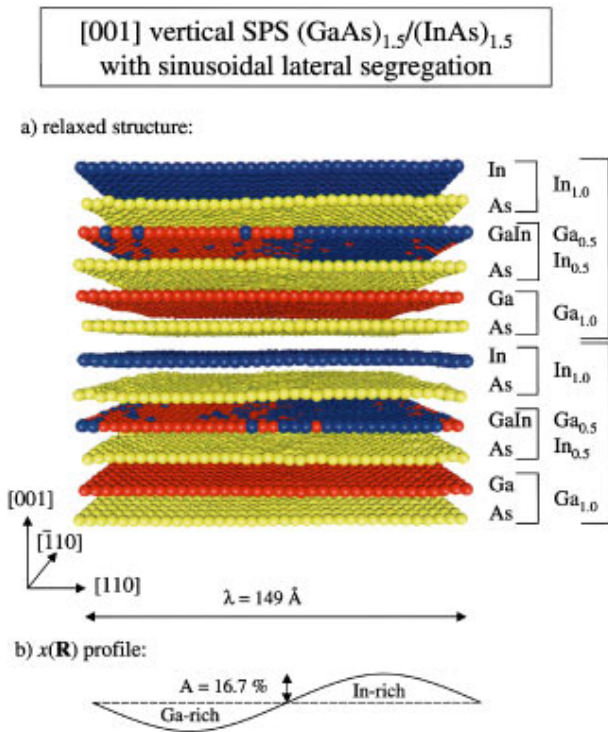


FIG. 1. The calculated minimum-energy atomic positions for $\text{Ga}_{0.5}\text{In}_{0.5}\text{As}$ system with SPS ($n=1.5$) and CM with $A=16.7\%$, $\lambda=149 \text{ \AA}$ and $\mathbf{u}=[110]$. The system consists of 25920 atoms of which only 8640 are shown (three of the total nine units cells in [001] direction). For clarity, distances in the [001] direction are magnified by a factor of 4. Yellow, red and blue spheres correspond to As, Ga and In atoms, respectively.

$[\bar{1}10]$ oriented atomic rows for each (001) plane. In this in-plane view we see contraction of the inter-row distance in the Ga-rich region (left) and an equivalent expansion in the In-rich region (right). This is consistent with the smaller covalent radius of Ga relative to the In atom. Surprisingly, all (001) planes behave nearly identically, i.e., the [110] in-plane displacements are *vertically phase-locked* between the different (001) planes despite the changing composition of these planes (ranging from pure layers to segregated mixed layers). Figures 2(c) and 2(d) show the out-of-plane [001] displacements of (001) planes in units of ideal monolayer separation (d_{001}). We see *significant buckling* which follows the composition wave and is largest for the As layers surrounding the segregated GaIn layer. In the absence of SPS (i.e., considering pure CM) our analysis shows no [001] buckling: the relaxation occurs only in the [110] direction and is analogous to Figs. 2(a) and 2(b). Thus, the significant effect of the combination of fractional period SPS and CM is to create height variations in addition to relaxation along the compositional wave.

Electronic structure: For each choice of lateral modulation profile $x(\mathbf{R})$ [Eq. (1)] and vertical SPS we solve the Schrödinger equation

$$\left(-\frac{1}{2}\nabla^2 + \sum_{\alpha,m} v_{\alpha}(\mathbf{r}-\mathbf{r}_{\alpha,m}; \mathcal{E}_{ij}) \right) \Psi_i(\mathbf{r}) = \epsilon_i \Psi_i(\mathbf{r}), \quad (2)$$

where $\mathbf{r}_{\alpha,m}$ are the strain-minimizing positions of atom species α (m running over individual atoms) and v_{α} is the screened atomic pseudopotential, fit¹⁷ to the measured bulk band structure and effective masses, as well as to the local

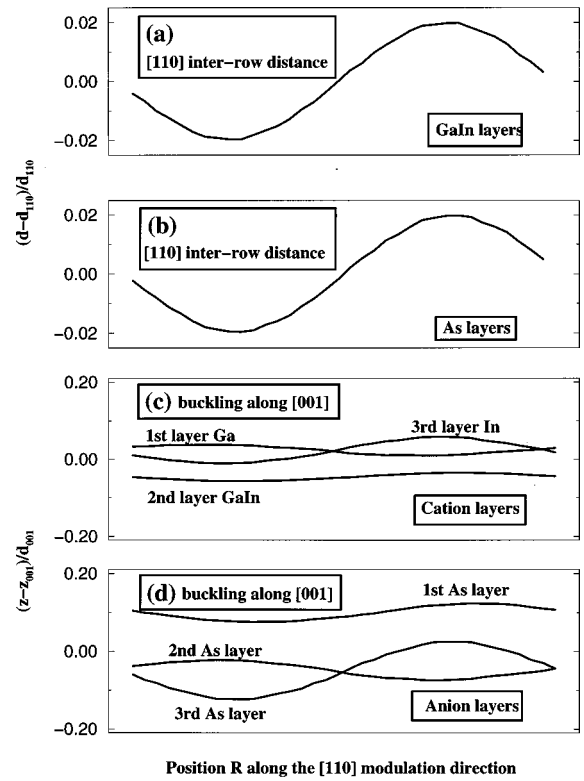


FIG. 2. The calculated atomic relaxations for the structure illustrated in Fig. 1. (a) and (b) in-plane displacements of the three cation layers and three anion layers, respectively, along the [110] CM direction, described by the inter-row distance $(d-d_{110})/d_{110}$ [where d_{110} is the distance in the unrelaxed (ideal) structure] between $[\bar{1}10]$ oriented atomic rows. All planes relax equally, showing thus vertical phase locking. (c) and (d) buckling of the (001) planes along the [001] z direction, described by the displacement $(z-z_0)/d_{001}$, where z and z_0 are vertical positions of the relaxed and ideal $[\bar{1}10]$ oriented rows, respectively, and d_{001} is the ideal monolayer separation in [001] direction.

density approximation (LDA)-calculated band offsets and deformation potentials. This potential depends analytically¹⁷ on the local strain tensor \mathcal{E}_{ij} , so as to reliably describe strain-modified band offsets and masses. The wave functions are expanded in plane waves.¹⁴ Equation (2) is diagonalized via the folded spectrum method¹⁴ whose computational cost scales only as the number of atoms N in the supercell (conventional methods scale as N^3 , thus restricting N to $\ll 10^3$ atoms).

Effects of CM on band structure: Figure 3 shows the effect of the composition modulation amplitude A on the valence bands (c), on the conduction band (b), and on the band gap (a); the reference (dashed horizontal line) is the equivalent $\text{Ga}_{0.5}\text{In}_{0.5}\text{As}$ supercell, where all cation sites are occupied randomly and relaxed. Figure 4 shows the corresponding wave function amplitudes for $A=16.7\%$. We see that CM+SPS split the valence band into the states V_1 , V_2 and V_3 , whose wave functions [Fig. 4(b)] are localized within the In-rich lateral domains. The conduction band minimum [Fig. 4(a)] is also localized within the In-rich domain. Hence, the $\{V_1, V_2, V_3\} \rightarrow \text{CBM}$ transitions are all “type I” (direct in coordinate and momentum spaces). The strong confinement of these hole states and electron state into the In-rich lateral channels (Fig. 4) defines the quantum wirelike characteristics of this system. The V_1-V_2 and

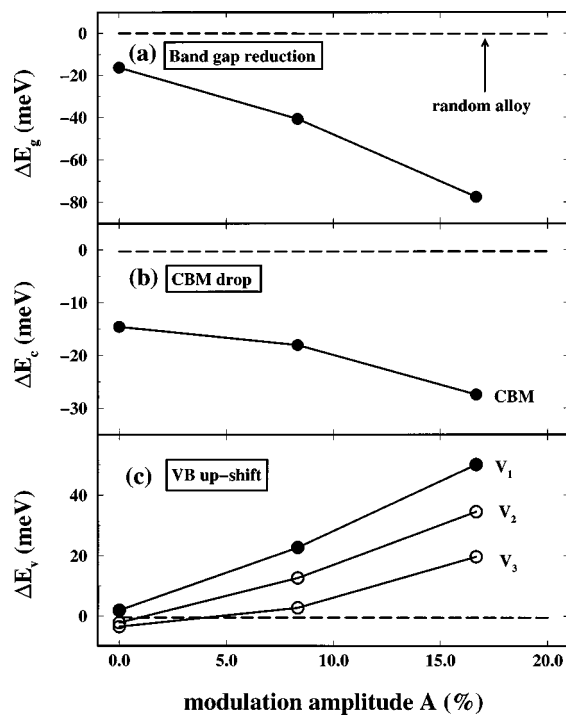


FIG. 3. Behavior of the valence and conduction band edges and the band gap as a function of the composition modulation amplitude A . The SPS+CM system is described by the parameters $n=1.5$, $\lambda=149$ Å and $\mathbf{u}=[110]$. $A=0.0$ corresponds to the $n=1.5$ SPS only with no CM, where the mixed GaIn is randomly occupied. The reference, illustrated by dashed lines, is the equivalent $\text{Ga}_{0.5}\text{In}_{0.5}\text{As}$ supercell with random occupation of all the cation sites. For the valence band, three uppermost levels are illustrated.

V_2 - V_3 valence band splitting are 16 and 14 meV for $A=16.7\%$ and increase with A . For $A=0$ (representing a $n=1.5$ SPS with no CM where the mixed GaIn layer is randomly occupied) the corresponding splittings are 4.1 and 1.3 meV. Figure 3 shows that CM+SPS act to raise the valence bands, lower the conduction band, and hence reduce the band gap. The calculated band-gap redshift for $\lambda=149$ Å, $\mathbf{u}=[110]$ and $n=1.5$ is shown in Fig. 3(a); it is ~ 40 (80) meV for $A\sim 8$ (16)%. For $A=0$ (SPS only) we find a band-

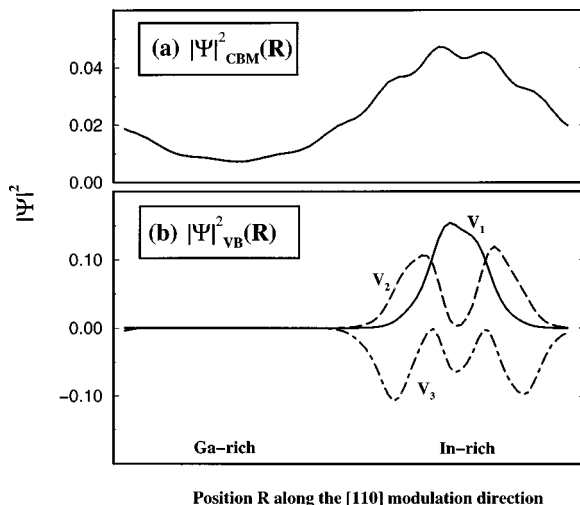


FIG. 4. The wave functions squared for the three uppermost valence states (a) and lowest conduction band (b) for the system described in Fig. 1. The 3D wave functions are projected first on the $[110]$ direction to allow a 1D representation. Smoothing is performed by averaging over four neighboring datapoints.

gap reduction of ~ 16 meV, indicating that the pure SPS structure induces a significant contribution to the redshift. Our calculations further reveal that the dependence of the redshift on CM wavelength λ is rather weak. On the other hand, the redshift *increases* as one goes from sinusoidal lateral modulation to square-wave lateral modulation (~ 10 meV for $A\sim 16\%$), and as one goes from integer-period SPS to fractional-period SPS (for $n=2$ SPS with the same CM parameters as for SPS $n=1.5$ we find a ~ 5 meV smaller redshift).

Effect of CM on polarization: (i) For pure $n=1.5$ [001] SPS we find the transition from the CBM to $V_1(V_2)$ to be polarized in the $[110]$ ($[\bar{1}10]$) direction. The transition probability to V_3 is small, and thus [001] polarization should not be detected among these lowest energy transitions. On the other hand, (ii) a pure $[110]$ CM creates $[\bar{1}10]$ -allowed transitions to V_1 and [001]-allowed transitions to V_3 (whereas the $[110]$ polarization is blocked). The transition to V_2 is forbidden. (iii) A *combination* of SPS+CM retains only the polarization allowed both for pure SPS and for pure CM, namely the $[\bar{1}10]$ to V_1 . This shows that SPS and CM act as sequential “filters”, each blocking a certain type of polarization. These results are consistent with the experimental observations^{2-4,7,9} showing that the polarized component perpendicular to the CM direction clearly dominates the parallel component.

This work was supported by the U.S. Department of Energy, Contract No. OER-BES-DMS, Grant No. DE-AC36-83-CH10093.

- ¹K. C. Hsieh, J. N. Baillargeon, and K. Y. Cheng, Appl. Phys. Lett. **57**, 2244 (1990).
- ²A. C. Chen, A. M. Moy, P. J. Pearah, K. C. Hsieh, and K. Y. Cheng, Appl. Phys. Lett. **62**, 1359 (1993).
- ³D. H. Rich, Y. Tang, and H. T. Lin, J. Appl. Phys. **81**, 6837 (1997).
- ⁴A. Mascarenhas, R. G. Alonso, G. S. Horner, S. Froyen, K. C. Hsieh, and K. Y. Cheng, Superlattices Microstruct. **12**, 57 (1992).
- ⁵K. Y. Cheng, K. C. Hsieh, and J. N. Baillargeon, Appl. Phys. Lett. **60**, 2892 (1992).
- ⁶S. T. Chou, K. Y. Cheng, L. J. Chou, and K. C. Hsieh, Appl. Phys. Lett. **66**, 2220 (1995).
- ⁷J. M. Millunchick, R. D. Twesten, S. R. Lee, D. M. Follstaedt, E. D. Jones, S. P. Ahrenkiel, Y. Zhang, H. M. Cheong, and A. Mascarenhas, MRS Bull. **22**, 38 (1997).
- ⁸J. M. Millunchick, R. D. Twesten, D. M. Follstaedt, S. R. Lee, E. D. Jones, Y. Zhang, S. P. Ahrenkiel, and A. Mascarenhas, Appl. Phys. Lett. **70**, 1402 (1997).
- ⁹J. M. Millunchick, R. D. Twesten, S. R. Lee, D. M. Follstaedt, E. D. Jones, S. P. Ahrenkiel, Y. Zhang, H. M. Cheong, and A. Mascarenhas, J. Electron. Mater. **26**, 1048 (1997).
- ¹⁰T. Y. Seong, A. G. Norman, I. T. Ferguson, and G. R. Booker, J. Appl. Phys. **73**, 8227 (1993).
- ¹¹S. W. Jun, T. Y. Seong, J. H. Lee, and B. Lee, Appl. Phys. Lett. **68**, 3443 (1996).
- ¹²A. Zunger and S. Mahajan, in *Handbook of Semiconductors*, 2nd ed., edited by S. Mahajan, (Elsevier, Amsterdam, 1994), Vol. 3, p. 1399.
- ¹³D. M. Wood and A. Zunger, Phys. Rev. B **53**, 7949 (1996).
- ¹⁴L.-W. Wang and A. Zunger, J. Chem. Phys. **100**, 2394 (1994); A. Zunger and L.-W. Wang, Appl. Surf. Sci. **102**, 350 (1996).
- ¹⁵C. Pryor, J. Kim, L.-W. Wang, A. Williamson, and A. Zunger, J. Appl. Phys. **83**, 2548 (1998).
- ¹⁶P. N. Keating, Phys. Rev. **145**, 637 (1966); R. M. Martin, Phys. Rev. B **1**, 4005 (1970).
- ¹⁷J. Kim, A. Williamson, S.-H. Wei, L.-W. Wang, and A. Zunger (unpublished).